Exclusive platination of loop adenines in the human telomeric G-quadruplex†

Hélène Bertrand,[a] Sophie Bombard,*[b] David Monchaud,[a] Eric Talbot,[a] Aurore Guédin,[c] Jean-Louis Mergny,[c] Renate Grünert,[d] Patrick J. Bednarski[d] and Marie-Paule Teulade-Fichou*[a]

Received 5th March 2009, Accepted 27th April 2009
First published as an Advance Article on the web 1st June 2009
DOI: 10.1039/b904599f

The present article reports on the platination of the human telomeric G-quadruplex by three Pt-terpyridine complexes. It is shown that extension of the aromatic surface of the terpyridine moiety surrounding the platinum atom influences both the binding affinity and the platination activity. Remarkably, the most strongly bound complex **Pt-ttpy** coordinates exclusively the adenine nucleobases present in the loop of the G-quadruplex. This exclusive single-site platination reflects the interaction of the compound with both the G-tetrad and the loop residues. In addition **Pt-ttpy** showed promising antiproliferative activity on a panel of cancer cell lines in a parallel study using cisplatin derivatives currently in clinical use.

Introduction

The telomeric overhang is an intracellularly stable single-stranded DNA, comprised of tandem repeats of the d[TTAGGG] sequence, which constitutes the very end of the human telomeres. The folding of this overhang into G-quadruplex structures, firmly established *in vitro*,[1] is suspected to inhibit cancer cell proliferation.[2] It is indeed hypothesized that G-quadruplex formation removes the protective proteins normally associated with telomeres (shelterin complex), which leads to genomic instability *via* telomere disorganization.[2] Hence, small molecules able to induce or stabilize G-quadruplexes are currently the subject of intense research efforts towards a fuller understanding of the function of telomeres *in vivo* in order to furnish new anti-cancer agents.[1–3]

In this context, the use of Pt(II) complexes as G-quadruplex binders was recently investigated. Two different classes of complexes can be found in the literature, according to their binding mode to the quadruplex. The first class is comprised of Pt(II) complexes used because their square planar geometry and cationic nature enable efficient π-stacking on the external G-quartet; this includes phenanthroline,[4] terpyridine,[5] dipyridophenazine,[6] phenanthroimidazole,[7] and bipyridine square[8] complexes. The second class is comprised of complexes that contain one or two labile ligands that enable metallic coordination to the G-quadruplex; this includes cisplatin,[9,10] *triamine*-platin,[11] a dinuclear platinum complex[11] as well as two intercalator-Pt(II) conjugates.[12,13] Interestingly, although some Pt(II) complexes from the first class possess one labile chloride ligand (*i.e.* phenanthroline and terpyridine series) their ability to platinate G-quadruplex has not yet been investigated. Hence, we report herein the platination ability of the terpyridine complexes previously developed by our group since some derivatives have shown good binding selectivity for the human telomeric quadruplex.[5] Additionally, several terpyridine derivatives described in the literature display promising cytotoxicity on several cancer cells lines that rival or surpass that of the clinically used cisplatin derivatives.[14]

Pt(II) compounds strongly coordinate the purine bases of DNA with a strong preference for guanine (N_7 of dG) and to a lesser extent for adenine (N_1 and N_7 of dA).[14] This ability is, of course, strongly dependent on the characteristics of the Pt derivative and the accessibility of the bases. It is worth distinguishing between divalent complexes that crosslink two bases (cis- or trans-platin) and monovalent complexes that coordinate a single site. It was shown that the divalent species have no selectivity for quadruplex-DNA but have been useful for probing the structure of the quadruplex-forming oligonucleotide 22AG that mimics the telomeric overhang, (d[$AG_3(T_2AG_3)_3$], Fig. 1).

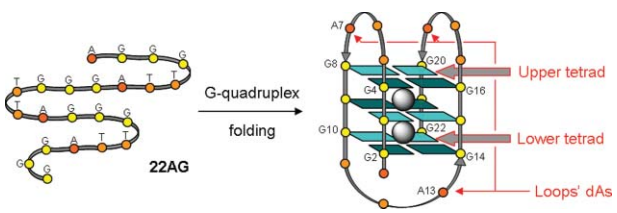

Fig. 1 Schematic representation of the folding of 22AG oligonucleotide into an anti-parallel G-quadruplex-DNA structure.

Of the monovalent compounds, three structurally different Pt(II) complexes have so far been tested on 22AG, the triamine-Pt ([$Pt(H_2O)(NH_3)_3]^{2+}$),[11] and two conjugates Pt-quinacridine (**Pt-MPQ**)[12] and Pt-acridine (**Pt-ACRAMTU**).[13] These studies have shown that both dAs present in the loops and dGs of external tetrads of the quadruplex can be platinated (Fig. 1). This

[a]*Institut Curie, Section Recherche, CNRS UMR176, Centre Universitaire Paris XI, Bât. 110, 91405, Orsay, France. E-mail: marie-paule.teulade-fichou@curie.fr; Fax: +33 1 6907 5381; Tel: +33 1 6986 3086*
[b]*Laboratoire de Chimie et Biochimie Pharmacologiques et toxicologiques, CNRS UMR8601, Université Paris Descartes, 45, rue des Saints-Pères, 75006, Paris, France. E-mail: sophie.bombard@parisdescartes.fr; Fax: +33 1 4286 8387; Tel: +33 1 4286 2256*
[c]*Muséum National dHistoire Naturelle (MNHN) USM 503 INSERM, U565, CNRS, UMR5153, 43, Rue Cuvier, Case postale 26, 75005, Paris, France*
[d]*Pharmazeutische/Medizinische Chemie, Institut für Pharmazie der Ernst-Moritz-Arndt-Universität Greifswald, Friedrich-Ludwig-Jahn-Straße 17, D-17487 Greifswald, Germany*

† Electronic supplementary information (ESI) available: NMR spectra and MS analyses of dbtpy and Pt-dbtpy; results of platination of [35G4/13GG] by Pt-tpy. See DOI: 10.1039/b904599f

observation was unexpected due to the participation of the N_7 of dG in the Hoogsteen H-bonding tetrad formation and is consistent with a certain degree of flexibility of the external G-quartets.[11] Furthermore, while platination of 22AG by triamine-Pt is essentially guided by the accessibility of the purines,[11] platination by the conjugates is strongly oriented by the binding site of the aromatic heterocyclic moiety. With Pt-acridine, in which the platinum complex is linked to the acridine unit by a short linker, the platination takes place on the dAs of the loops (50%) and on dGs (50%) that have not been identified so far.[13] Conversely, with Pt-quinacridine only dGs of the lower tetrad are platinated. Since, in this case, the platinum species and the quinacridine unit are associated through a long and flexible linker, this might indicate binding of the aromatic heterocyclic moiety on the opposite (upper) tetrad.[12]

Results and discussion

We have recently developed a set of Pt-terpyridine complexes which exhibit affinity and selectivity towards the telomeric G-quadruplex.[5,15] Two of these compounds (Fig. 2) differ according to the structure of the terpyridine moiety, which is either a simple terpyridine (tpy) or a *p*-tolyl-terpyridine (ttpy). Additionally, in the hope to optimize the π–π stacking interactions between the aromatic ligand and the quadruplex, we decided to synthesize a third derivative that contains an aromatically extended terpyridine, **Pt-dbtpy** (Fig. 2). Given that, in this series, the platinum atom is directly coordinated to the aromatic ligand *i.e.* the terpyridine core, that is assumed to act as the G-quartet-interacting moiety, elucidating the platination profile of these complexes may provide an insight into the nature of the interaction. It was also of interest to compare the platination ability of this terpyridine series with that of the above-mentioned monovalent platinum derivatives.

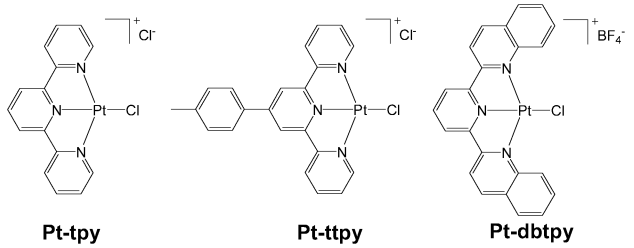

Fig. 2 Chemical structure of Pt(II)-complexes used in this study.

Synthesis of Pt-dbtpy

The synthesis of **Pt-dbtpy** requires the synthesis of a dibenzoterpyridine (dbtpy), in which two benzene rings are fused to the lateral pyridine rings. The pentacyclic unit dbtpy was obtained *via* a double Friëdlander condensation between 2,6-diacetylpyridine and 2-aminobenzaldehyde (Fig. 3). The latter was prepared *in situ* by iron powder-mediated reduction of 2-nitrobenzaldehyde. Finally, the platinum complex **Pt-dbtpy** was synthesized by mixing the dbtpy with K_2PtCl_4 in the presence of $NaBF_4$, with a moderate chemical yield (21%).

Quadruplex affinity and selectivity

The quadruplex affinity of **Pt-tpy** and **Pt-ttpy** as well as their selectivity with regard to duplex-DNA have been previously

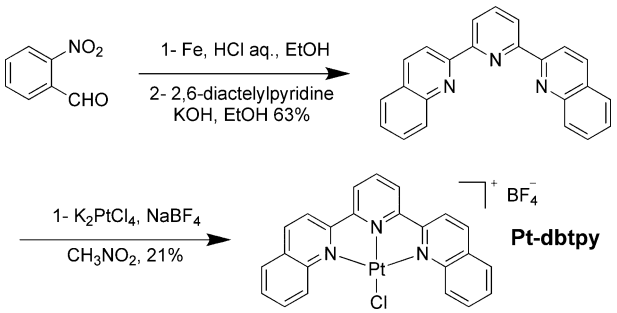

Fig. 3 Synthesis of **Pt-dbtpy**.

evaluated through FRET-melting and G4-FID assays.[5,15] The FRET-melting assay is based on the thermal denaturation of a quadruplex-forming oligonucleotide, F21T (*FAM*-$G_3[T_2AG_3]_3$-*Tamra*), labelled at its extremities by a FRET D/A pair (FAM for 6-carboxy-fluorescein in 5′ position as a donor and TAMRA for 6-carboxy-tetramethylrhodamine in 3′ position as acceptor).[16]

The melting of F21T is then followed by fluorescence spectroscopy, and the ability of each compound to increase the melting temperature ($T_{1/2}$) of the F21T quadruplex is correlated to its affinity for the DNA target. This ability is quantified by $\Delta T_{1/2}$ values, defined as $\Delta T_{1/2} = T_{1/2}(+\text{ligand}) - T_{1/2}(-\text{ligand})$.[16] This assay also enables the evaluation of the compound's selectivity for quadruplex-DNA with regard to duplex-DNA, by comparing the $\Delta T_{1/2}$ values determined in the absence or presence of a large excess of duplex-DNA (ds26). This selectivity is quantified by ^{FRET}S values, defined as $^{FRET}S = \Delta T_{1/2}(+ds26)/\Delta T_{1/2}(-ds26)$ ($^{FRET}S \rightarrow 1$ for selective ligands).[16,17] The stabilization imparted by **Pt-dbtpy** ($\Delta T_{1/2} = 8.0$ °C, Fig. 4A) is better than that of **Pt-tpy** ($\Delta T_{1/2} = 1.1$ °C) but lower than that of **Pt-ttpy** ($\Delta T_{1/2} = 11.3$ °C);[5,15] this indicates that the extension of the aromatic surface of the tpy moiety that surrounds the platinum atom leads to enhancement of the quadruplex-affinity, but to a lesser extent than expected. However, in terms of quadruplex selectivity, identical results were obtained for **Pt-ttpy** and **Pt-dbtpy** ($^{FRET}S = 0.80$ in the presence of 3 μM of ds26, Fig. 4A), indicating that the broader dbtpy neither improves nor alters the selectivity imparted by ttpy.

The G4-FID assay is based on the displacement of the fluorescent probe thiazole orange (TO) by a given ligand, from DNA matrices.[15] When performed with 22AG, the TO displacement ability reflects the quadruplex affinity quantified by $^{G4}DC_{50}$ values, *i.e.* the concentration required to displace 50% of the TO from the quadruplex matrix ($^{G4}DC_{50} \rightarrow 0$ for affinic ligands).[15] The G4-FID also permits evaluation of the quadruplex selectivity, by measuring the ability of the ligand to displace TO from a duplex-DNA matrix (ds26), quantified by $^{ds}DC_{50}$ values. The global selectivity is then calculated as $^{G4\text{-}FID}$Sel. values, defined as $^{FID}Sel. = {}^{ds}DC_{50}/{}^{G4}DC_{50}$.[15] The TO displacement ability of **Pt-dbtpy** ($^{G4}DC_{50} = 0.53$ μM, Fig. 4B) is intermediate between **Pt-tpy** ($^{G4}DC_{50} = 1.46$ μM) and **Pt-ttpy** ($^{G4}DC_{50} = 0.18$ μM).[5,15] In terms of quadruplex selectivity, a $^{G4\text{-}FID}$Sel. value of 10 was found for **Pt-dbtpy**, which is identical to that determined for **Pt-ttpy**. Globally, these results corroborate the FRET-melting observations.

Altogether, the data obtained from the two assays demonstrate that extending the aromatic surface of the terpyridine unit significantly increases the G-quadruplex affinity. However, it is clear that adding a tolyl group on the backside of the tpy (ttpy) is more

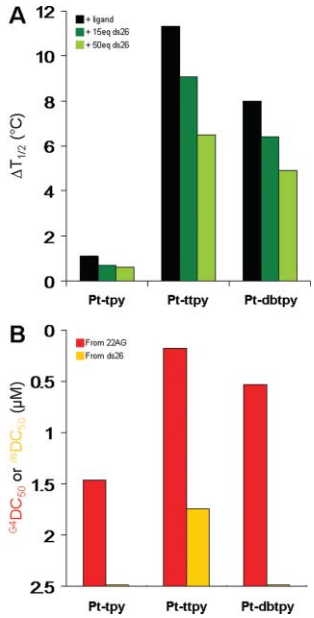

Fig. 4 A. Diagrammatic bar representation of FRET-melting results. Experiments are performed with F21T (0.2 μM) in presence of 1 μM of ligand without (black bar) or with 3 μM (deep green bar) and 10 μM (light green bar) of competitive ds26, in 10 mM lithium cacodylate + 100 mM NaCl. B. Diagrammatic bar representation of G4-FID results. DC_{50} values determined for G4-FID experiments carried out with 22AG (red bar) or ds26 (yellow bar) with increasing amount of ligand (from 0 to 2.5 μM), in 10 mM sodium cacodylate + 100 mM KCl.

efficient than increasing the hindrance of the frontside (dbtpy), the former probably providing a more suitable combination between π-surface and steric hindrance for fitting into the target.

Quadruplex platination

The platination of 22AG by **Pt-tpy**, **Pt-ttpy** and **Pt-dbtpy** complexes was then investigated by means of denaturing gel electrophoresis and 3′-exonuclease experiments.[9,11] The three Pt-derivatives were firstly incubated with pre-folded 5′-end radiolabelled 22AG (drug/DNA= 1/1 to 3/1, 100 μM) in either sodium- or potassium-rich conditions (50 mM $NaClO_4$ or $KClO_4$, pH 5.2, 16 h, 37 °C), given that the quadruplex-structure of 22AG is highly dependent on the nature of its cationic environment.[1] The mixtures were then analyzed by polyacrylamide gel electrophoresis in denaturing conditions (Fig. 5). In Na^+ conditions, two major retarded bands were detected with **Pt-tpy** (b1 and b2, Fig. 5) while only one was found with **Pt-ttpy** (a1, Fig. 5). These results indicate that one (**Pt-ttpy**) or two (**Pt-tpy**) platinated adducts are the main species obtained. However, no platination was detected with **Pt-dbtpy**, thus indicating that the broader π-surface of this ligand hampers the platination. This probably originates in the steric hindrance imparted by the two additional benzene rings that closes the access of the nucleobases to the platinum cation.

The platination sites were then determined for adducts obtained with **Pt-tpy** and **Pt-ttpy**. To this end, the various adducts detected on the gel shown in Fig. 5 were isolated and the platination sites analyzed *via* 3′-exonuclease digestion.[9,11] The digestion of the adduct present in band a1 showed a single pausing site (band a1′, Fig. 5A1), thus indicating that only one base of 22AG was platinated. Band a1′ was then deplatinated *via* NaCN treatment (Fig. 5A2) and the length of the deplatinated fragment was determined using denaturing gel electrophoresis against a partially digested 22AG.[9,11] This allows identification of the pausing site of the 3′-exonuclease and, therefore, that of the platinated nucleobase. A_{13} was identified, showing that the adduct of band a1 actually corresponds to 22AG platinated on A_{13} by **Pt-ttpy** (~35% yield, average of four experiments). The same gel analysis sequence was repeated with the platinated species obtained with **Pt-tpy** (Fig. 5B1 and 5B2). In this case, the adduct of band b1 corresponds to 22AG platinated on A_7 (~40% yield) and band b2 corresponds to 22AG diplatinated on A_7 and A_{13} (~30% yield), the migration of products of band b2 being slower since the velocity of migration decreases with the number of platinum adducts.

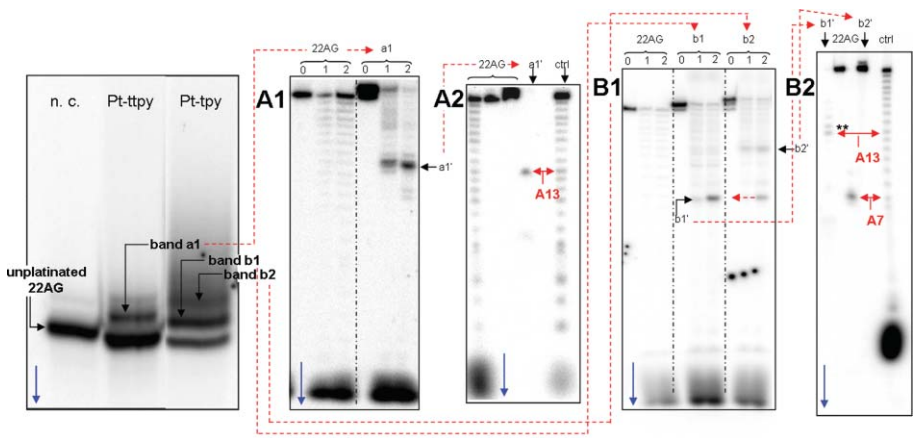

Fig. 5 Electrophoresis gel analysis sequence of 22AG platination products by **Pt-tpy** and **Pt-ttpy**. Left. Analysis for the platination of 22AG structured in G-quadruplex in Na+ conditions by **Pt-tpy** and **Pt-ttpy** (n.c. for no complexes); A1,B1. 3′-exonuclease digestion of bands a1 (A1) and b1 and b2 (B1) (isolated from platination gel shown on the left) with two different enzymatic concentrations (1 and 2, 0 for no enzymes); A2,B2. Determination of platination sites of digestion arrests a1′ (A2) and b1′ and b2′ (B2) (isolated from gels A1 and B1 respectively) after NaCN treatment; ctrl corresponds to the partial digestion fragments of non-platinated 22AG, with an enzyme dilution of 0.001u/μL; it provides the reference scale for the migration of the deplatinated digested fragments. ** indicates the remaining non-deplatinated fragment after NaCN treatment. Blue arrow indicates migration sense.

Intriguingly, we obtained identical platination products in potassium buffer indicating that the platination pattern is independent of the ionic conditions (Na^+ *vs.* K^+, not shown). This was unexpected given that the nature of the cation strongly influences the quadruplex topology.[1] It is now generally agreed that the main structure of 22AG in Na^+ conditions is basket-type (Fig. 1).[1,18] Its structure in presence of K^+ is still debated, but the current consensus considers that 22AG is a mixture of hybrid-type structures in K^+.[1,19] Given that the platination pattern of 22AG by Pt(II)-complexes is similar in both cationic environments, Pt complexes could interact preferentially with a basket-type quadruplex, resulting in its covalent trapping.

Circular dichroism studies

This hypothesis was verified by circular dichroism (CD) spectroscopy, a very powerful technique for monitoring the influence of the binding of a ligand to a quadruplex structure.[20,21] 22AG folded in K^+- or Na^+-rich conditions has been shown to adopt distinct topologies (hybrid-type and anti-parallel structures respectively), which are characterized by distinct CD signatures. A quadruplex with a hybrid-type structure (*i.e.* with a combination of *syn* and *anti* glycosidic angles, Fig. 6A) is generally characterized by an ellipticity (Θ) maximum at 295 nm and a shoulder near 268 nm (Fig. 6A) while the anti-parallel structure (with a different combination of the *syn* and *anti* angles, Fig. 6B) has two maxima at 295 (positive) and 264 nm (negative).[20] Upon addition of increasing amounts of **Pt-ttpy** (from 0 to 5 equiv., from black to purple curves, Fig. 6), CD spectra highlight that the binding of **Pt-ttpy** to the K^+-favoured hybrid-type quadruplex (Fig. 6A) leads to a profound reorganisation of the quadruplex-structure, the final quadruplex/ligand complex being characterized by a CD signal typical of the anti-parallel conformation of 22AG. On the other hand, **Pt-ttpy** interacts also with the Na^+-favoured basket-type

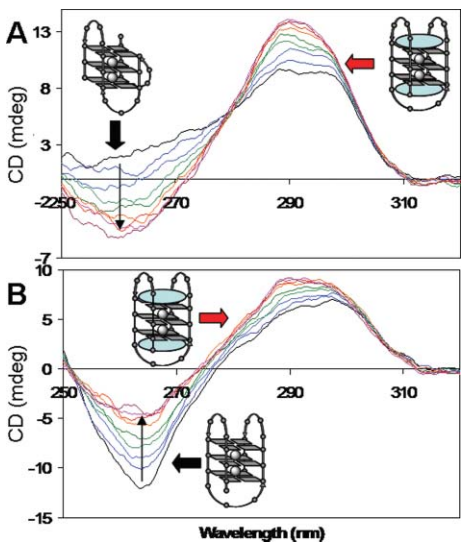

Fig. 6 CD analysis of the interaction between 22AG and **Pt-ttpy**. Modification of the CD signal of 22AG (3 μM) upon addition of increasing amounts of **Pt-ttpy** (from 0 (black curve) to 5 equiv. (violet curve)) in sodium cacodylate buffer 10 mM plus 100 mM KCl (A) or NaCl (B). Black and red arrows indicate the starting quadruplex and the final complex respectively.

22AG quadruplex (Fig. 6B), as demonstrated by the modification of the intensity of the CD signal, but without modifying the overall shape of its CD signature. These results demonstrate that Pt-complexes interact preferentially with the anti-parallel quadruplex, and explain why the platination results obtained by electrophoresis gel analysis are identical in both cationic conditions. We thus selected the anti-parallel conformation of 22AG to interpret the platination results in terms of ligand binding sites.

Selectivity of platination

Given that **Pt-ttpy** has been shown to interact selectively with quadruplex-DNA by both FRET-melting and G4-FID assays, it was thus of interest to determine if this Pt-complex could selectively platinate a quadruplex motif in the presence of a duplex-DNA. To this purpose, we decided to use an intramolecular platination competition system in which both duplex and quadruplex parts are present (Fig. 7). This system, already used in previous studies,[9,12] consists of a 35-nucleotide DNA strand (35G4, grey strand, Fig. 7) in which the sequence of 22AG (responsible for the quadruplex part) is flanked by a 13-nucleotide tail; the duplex part is formed by the association of this tail with the complementary 13-nucleotide DNA (13GG, black strand, Fig. 7). In the resulting system [35G4/13GG] two possible platination sites are present on each DNA architecture: A_7 and A_{13} on the quadruplex part and G_6 and G_7 on the duplex part. The platination by **Pt-ttpy** (80 μM) was carried out using the [35G4/13GG] system. This system, which has been calibrated with cisplatin,[9] is based on comparison of platination of dGs in a duplex architecture and dAs in the single strand of the quadruplex loops. The monitoring of the disappearance (and so the platination) of both moieties (Fig. 8A and B) demonstrates that 13GG is platinated to a very small extent during the course of the study (~5% of platination after 600 min of reaction) while 35GG reacts to a far greater extent (~40% of platination after 600 min of reaction) (Fig. 8C). The ratio of the rate constants of both DNA strands (k_{35G4}/k_{13GG}) can be calculated as already described, following the equation: $k_{35G4}/k_{13GG} = \ln([35G4]/[35G4]_{t=0})/\ln([13GG]/[13GG]_{t=0})$ (Fig. 8D). The value obtained (~12) is higher than those observed for *cis*-Pt and **Pt-MPQ** (~2 and ~6 respectively)[9,12] and for **Pt-tpy** (~5, see ESI†)

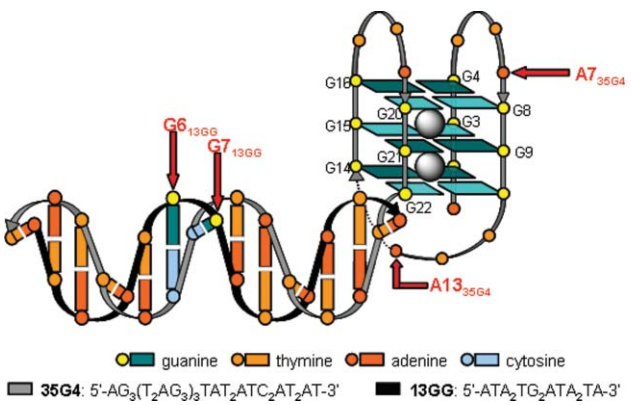

Fig. 7 Schematic representation of the [35G4/13GG] system, with 35G4 (d[$AG_3(T_2AG_3)_3TAT_2ATC_2AT_2AT$]) and 13GG (d[$ATA_2TG_2ATA_2TA$]) as grey and black strands respectively. Red arrows indicate the platinable nucleobases.

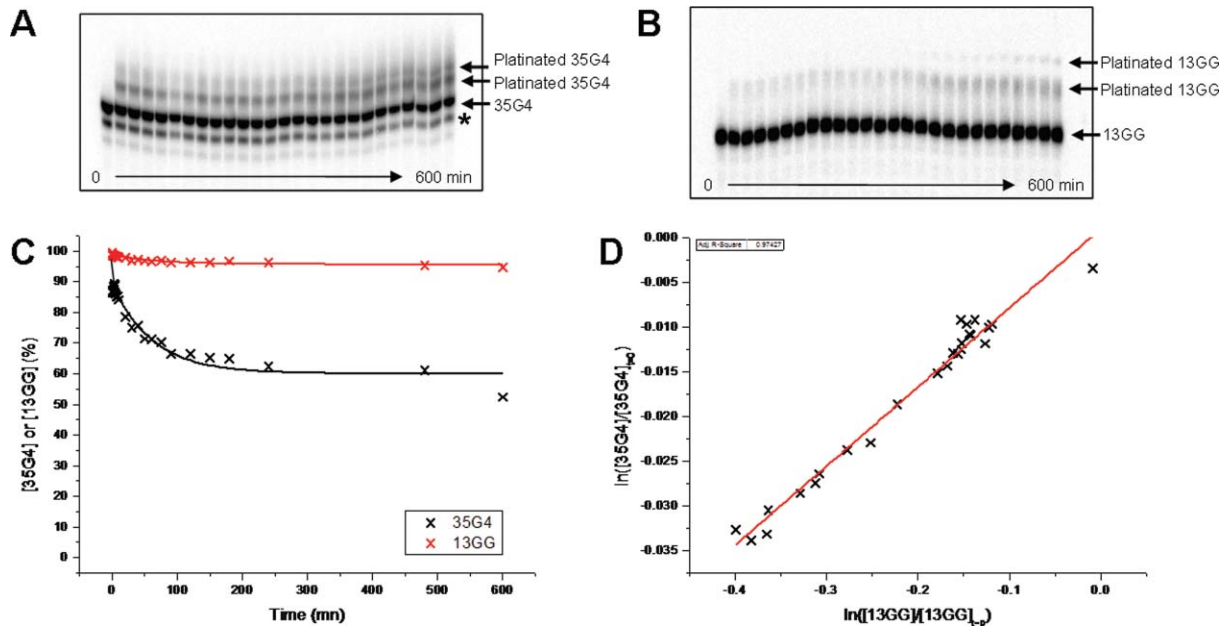

Fig. 8 Denaturing gel electrophoresis of the kinetics of platination of the [35G4/13GG] system (100 μM) by **Pt-ttpy** (80 μM) with radiolabelled 35G4 (A) or 13GG (B). Concentration of remaining 35G4 (black crosses, from the gel A) or 13GG (red crosses, from the gel B) reported as a function of the time (C). Experimental determination of the rate constants ratio (k35G4/k13GG) of the quadruplex- *vs.* duplex-DNA platination (D). * indicates a 34-nucleotide DNA strand deriving from 35G4 that remains after purification.

clearly indicating that platination by **Pt-ttpy** preferentially occurs on the quadruplex part.

Cell growth inhibition properties

We thus decided to further evaluate the potential of these Pt(II)-complexes as anti-tumour agents by studying their effects on the growth of a representative panel of cancer cell lines, namely MCF-7 (human breast cancer), RT-4 and 5637 (two human bladder cancers), DAN-G (human pancreas cancer) and A-427 and LCLC-103H (two human lung cancers).[22] Their efficiency was compared to that of clinically used candidates (cisplatin, oxaliplatin, DACH-Pt and carboplatin).[14] As seen in Table 1, the antiproliferative activity obtained for these complexes toward five of the six tested cell lines is promising (MCF-7 cell line has been found insensitive to both **Pt-tpy** and **Pt-ttpy**) and results of **Pt-ttpy** are generally better than that of **Pt-tpy** (except for the RT-4 cell line). Most interestingly, in all cell lines, **Pt-ttpy** is more efficient than carboplatin.[14] Even if these results are encouraging for further developments of extended terpyridine Pt complexes as antiproliferative agents, they are still to be considered as preliminary. Indeed the link between the cellular cytotoxicity and a process involving the platination of the human telomeric G-quadruplex has yet to be proven.

Conclusions

In the present study we have shown that the two terpyridine platinum complexes **Pt-tpy** and **Pt-ttpy** react exclusively with two dAs (either A_7 or A_{13}, or both) located in the loops of the quadruplex formed in the human telomeric sequence. **Pt-ttpy** is likely to interact by stacking on external G-tetrads;[5] it will trap only bases situated in its very close vicinity, *i.e.* dAs in surrounding loops. Given that **Pt-ttpy** coordinates the A_{13} residue exclusively, it can be concluded that this compound interacts mainly with the lower tetrad, therefore interacting with dA of the diagonal loop. This is consistent with participation of the nucleobases of this loop to the stabilization of the ligand binding, as already

Table 1 Growth inhibition properties (IC_{50} (μM)) of **Pt-tpy**, **Pt-ttpy**, cisplatin, oxaliplatin, DACH-Pt and carboplatin against a representative panel of human cancer cell lines

	bladder		lung		pancreas	breast
	5637	RT-4	A-427	LCLC-103H	DAN-G	MCF-7
cisplatin	0.35 ± 0.10[a]	1.61 ± 0.16	1.96 ± 0.54	0.90 ± 0.19	0.73 ± 0.34	1.38 ± 0.29
oxaliplatin	1.13 ± 0.33	0.16 ± 0.01	0.76 ± 0.08	0.51 ± 0.32	22.58 ± 6.6	0.32 ± 0.04
DACH-Pt	0.82 ± 0.19	0.17 ± 0.11	0.93 ± 0.27	0.57 ± 0.23	0.95 ± 0.74	0.23 ± 0.13
carboplatin	4.34 ± 1.70	29.03 ± 18.8	25.28 ± 4.0	14.59 ± 5.6	12.79 ± 6.8	29.4 ± 9.8
Pt-tpy	5.98 ± 2.72	3.85 ± 0.53	2.08 ± 0.86	2.73 ± 0.66	1.62 ± 0.29	27.2 ± 6.4
Pt-ttpy	3.11 ± 1.21	8.20 ± 1.70	1.17 ± 0.37	1.77 ± 0.81	0.52 ± 0.13	>20

[a] IC_{50} values (μM) are given with standard deviations; see the experimental part and ref. 22 for the protocol used to determine these values.

reported for acridine or porphyrine derivatives.[23] In contrast, **Pt-tpy** was found to be a poor quadruplex binder,[5,15] but it platinates A_7 with high efficiency (along with A_{13} as a minor event); given that A_7 has already been shown to be the most accessible dA of the 22AG quadruplex,[9,11] this suggests that **Pt-tpy** platinates A_7 without tetrad interaction.

This study demonstrates that elucidating the platination profile of 22AG by Pt(II)-complexes can provide insights into the binding mode of these complexes with G-quadruplexes. In the present case, the tetrad-interacting compound **Pt-ttpy** preferentially interacts with the lower tetrad which is surrounded by a diagonal loop (Fig. 9), which may in turn play a part in the compound interaction. This interaction leads to the subsequent platination of the dA that is the most accessible from that position, *i.e.* A_{13}. On the other hand, the compound with low tetrad-interacting ability **Pt-tpy** platinates preferentially A_7, the dA from a lateral loop that surrounds the upper tetrad, because A_7 is the most reactive to platination (Fig. 9). In summary, we have shown that the present terpyridine complexes are the first platinum derivatives able to coordinate the loop adenines of the 22AG G-quadruplex exclusively. Remarkably, this is in contrast with the platination profiles observed with other Pt-derivatives published to date. This selectivity has been proposed to be governed mainly by the predominant binding of the compound *via* stacking on external tetrads, which allows the trapping of the adenine in the vicinity. This study also demonstrates that the platination efficiency of the tpy-based Pt(II)-complexes is highly dependent on the accessibility of the platinum atom, given that the use of the extended dibenzoterpyridine (dbtpy) leads to inactive species. Additionally, the high efficiency of the reaction outlines the possibility of trapping the quadruplex form with specifically tailored monovalent Pt(II) complexes that induce strong Pt-adenine coordination. This could be of interest for telomere-targeted anti-tumour activity as suggested by preliminary results obtained on the inhibition of the growth of cancer cells. Finally the study of G-quadruplex platination could also offer an interesting tool to probe the accessibility of loop residues providing an entry to distinguish between various quadruplexes differing by loop length and sequence.

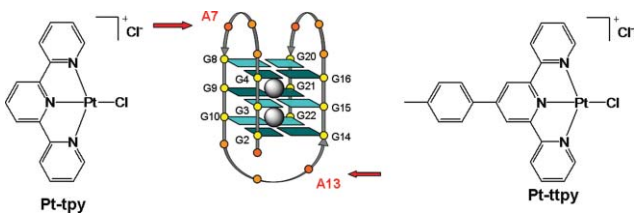

Fig. 9 Schematic representation of the platination patterns of 22AG by **Pt-tpy** and **Pt-ttpy**.

Experimental

Materials and methods

^{1}H and ^{13}C spectra were recorded on a Bruker Avance 300 using TMS as internal standard. Deuterated solvents ($CDCl_3$ and DMSO-d_6) were purchased from SDS. The following abbreviations are used: singlet (s), doublet (d), triplet (t) and multiplet (m). For mass spectrometry, ES is used as an abbreviation of electrospray. Reagents and chemicals were purchased from Sigma-Aldrich unless otherwise stated. Solvents were purchased from SDS. Dichloromethane (CH_2Cl_2), ethanol (EtOH) and methanol (MeOH) were distilled from calcium hydride, diethyl ether (Et_2O) was distilled from sodium. UV-Vis absorption spectra were recorded on a Secoman Uvikon XL spectrophotometer, fluorescence emission spectra were recorded on a Jobin Yvon FluoroMax-3 spectrophotometer at 20 °C, fluorescence melting curves on a Stratagene Mx3000P real-time PCR machine and CD spectra on a JASCO J-710 circular dichroism spectropolarimeter.

Synthesis of Pt-dbtpy

dbtpy. To a solution *o*-nitrobenzaldehyde (151 mg, 1.0 mmol, 2.0 equiv) in ethanol (10 ml) is added iron powder (223 mg, 4.0 mmol, 4.0 equiv.) followed by 0.1 N aq. HCl (0.5 ml, 0.05 mmol, 0.05 equiv.). The resulting mixture is vigorously stirred at 95 °C (oil bath) for 1 h 30 min. 2,6-Diacteylpyridine (310 mg, 2.0 mmol, 2.0 equiv.) and KOH (111 mg, 2.0 mmol, 2.0 equiv.) are then added. The reaction mixture is stirred at 95 °C for 1 h, then cooled to room temperature, diluted with CH_2Cl_2 (100 ml) and filtered through a celite pad. The solution is concentrated and the residue is washed with methanol that leads to the appearance of a solid, which is collected by filtration and dried under reduced pressure to give **dbtpy** as a white solid (209 mg, 63% chemical yield). ^{1}H-NMR (300 MHz, $CDCl_3$): δ (ppm) 8.85 (d, J = 8.4 Hz, 2H), 8.77 (d, J = 7.8 Hz, 2H), 8.34 (d, J = 8.5 Hz, 2H), 8.21 (d, J = 8.4 Hz, 2H), 8.07 (t, J = 7.8 Hz, 1H), 7.88 (d, J = 8 Hz, 2H), 7.76 (app. t, J = 7.15 Hz, 2H), 7.57 (app t, J = 7.33 Hz, 2H); ^{13}C-NMR (75 MHz, $CDCl_3$): δ (ppm) 156.6, 155.9, 148.3, 138.6, 137.1, 130.2, 129.9, 128.7, 128.0, 127.2, 122.5, 119.5; LRMS (ES^+): *m/z* 334.17 ($[M + H]^+$, 100%).

Pt-dbtpy. A solution of K_2PtCl_4 (42 mg, 0.1 mmol, 1.0 equiv.), **dbtpy** (33 mg, 0.1 mmol, 1.0 equiv.), $NaBF_4$ (22 mg, 0.2 mmol, 2.0 equiv.) in dry $MeNO_2$ (4 ml) is thus stirred and heated to 100 °C under nitrogen and protected from light for 48 h. The resulting suspension is filtered on a membrane (Schleicher & Schuell, 1 μm); the resulting orange solid is washed with CH_2Cl_2 and Et_2O to afford **Pt-dbtpy** (14 mg, 21% chemical yield). ^{1}H-NMR (300 MHz, DMSO-d_6): δ (ppm) 8.90 (d, J = 8.4, 2H), 8.76 (d, J = 7.5 Hz, 2H), 8.62 (d, J = 8.6 Hz, 2H), 8.26 (t, J = 7.4 Hz, 1H), 8.17 (d, J = 8.2 Hz, 2H), 8.10 (d, J = 7.8 Hz, 2H), 7.87 (t, J = 7.0 Hz, 2H), 7.70 (d, J = 7.1 Hz, 2H). LRMS (ES^+): *m/z* 527 ($[M - Cl]^+$, 100%, 555 $[M - Cl + CN]^+$, 80%, 563.9 $[M]^+$, 5%. Traces of free ligand dbtpy were detected in the NMR spectrum (estimated 10% as seen from ESI). However, due to instability of the complex in HPLC conditions, it could not be purified and thus was tested as is.

FRET-melting assay

The FRET-melting protocol has been thoroughly described in ref. 16. Labelled oligonucleotide is purchased from Eurogentec (Belgium); after an initial dilution at 100 μM concentration in purified water, further dilutions are carried out in the relevant buffer. FRET assay is performed as a high-throughput screen in a 96-well format, with F21T (*FAM*-$G_3[T_2AG_3]_3$-*Tamra*, with *FAM*: 6-carboxyfluorescein and *Tamra*: 6-carboxy-tetramethylrhodamine). Fluorescence melting curves were

determined with a Stratagene Mx3000P real-time PCR machine, using a total reaction volume of 25 µL, with 0.2 µM of tagged oligonucleotide in a buffer containing 10 mM lithium cacodylate pH 7.2 and 100 mM NaCl. After a first equilibration step at 25 °C during 5 minutes, a stepwise increase of 1 °C every minute for 71 cycles to reach 95 °C was performed and measurements were made after each "cycle" with excitation at 492 nm and detection at 516 nm. The melting of the G-quadruplex was monitored alone or in the presence of various concentrations of compounds and/or of double-stranded competitor ds26 (5′-CAATCGGATCGAATTCGATCCGATTG-3′). Final analysis of the data was carried out using Excel and Kaleidagraph software. Emission of FAM was normalized between 0 and 1, and $T_{1/2}$ was defined as the temperature for which the normalized emission is 0.5. $\Delta T_{1/2}$ values are mean of 2 to 4 experiments ± standard deviation.

G4-FID assay

The G4-FID protocol has been thoroughly described in ref. 15. A temperature of 20 °C is kept constant with thermostated cell holders. Each experiment is performed in a 10 mm path length quartz cuvette, in 10 mM sodium cacodylate buffer pH 7.4 with 100 mM KCl, in a total volume of 3 mL. The G4-FID assay is designed as follows: 0.25 µM pre-folded DNA target is mixed with thiazole orange (0.50 µM for 22AG, 0.75 µM for ds26). Each ligand addition step (from 0.5 to 10 equivalents) is followed by a 3 min equilibration period after which the fluorescence spectrum is recorded. The percentage of displacement is calculated from the fluorescence area (FA, 510–750 nm, $\lambda_{ex} = 501$ nm), using: percentage of displacement $= 100 - [(FA/FA_0)\times 100]$, FA_0 being the fluorescence of TO bound to DNA without added ligand. The percentage of displacement is then plotted as a function of the concentration of added ligand.

In terms of quadruplex selectivity, given that **Pt-dbtpy** is not able to displace 50% of TO from ds26 (so, no $^{ds}DC_{50}$ can be determined), the selectivity has to be estimated on the basis of the displacement obtained with 2.5 µM of **Pt-dbtpy** ($^{ds}C_{2.5\,\mu M} = 27\%$) and the concentration of **Pt-dbtpy** required to displace the same percentage of TO from quadruplex ($^{G4}C = 0.25\,\mu M$); the selectivity can thus be estimated, using the equation $^{G4\text{-}FID}Est.Sel. = 2.5/^{G4}C$, which leads to an $^{G4\text{-}FID}Est.Sel.$ value of 10.

Electrophoresis gel protocol and analysis sequence

5′-end-labeling of oligonucleotides. 22AG (d[$AG_3(T_2AG_3)_3$]) was synthesised and purified by Eurogentec, desalted on a Sephadex G25 column and stored at –20 °C as a 1 mM aqueous solution. The oligonucleotide was 5′-end-labeled using polynucleotide kinase (Pharmacia Biotech) and [γ^{32}P]ATP (Pharmacia Biotech). The reaction products were purified on 20% denaturing gel electrophoresis and desalted on a Sephadex G25 column. The various platination products were quantified using a STORM 960 Phosphorimager with the Imagquant software for data processing.

Platination experiments of 22AG. 5′-end radiolabeled 22AG was mixed with 100 µM of non-radiolabeled material in 50 mM $NaClO_4$ or $KClO_4$ solution, heated at 90 °C for 5 min and allowed to reach 20 °C (2 h) to induce the formation of quadruplex structure. It was then incubated with 100 µM of ligand for 16 h at 37 °C.

Determination of the platinum binding sites by 3′-exonuclease digestion. 3′-exonuclease is usually employed to determine the platination sites of oligonucleotides since its digestion is stopped by platinum mono-adducts. The platinated products, isolated from gel electrophoresis, were incubated in 10 mM Tris-HCl buffer (pH 8.0), in the presence of 2 mM $MgCl_2$ and 0.5mg/mL t-RNA with the 3′-exonuclease phosphodiesterase I from crotalus adamanteus venom (UBS) at 0.04 u/µL for 30 min at 37 °C. The partial digestion of non-platinated oligonucleotide was run with 0.001 u/µL. The digested fragments were purified on a 20% denaturing gel. The migration of the fragments depends on the presence of platinum adducts; therefore, each of them has been eluted from the gel, precipitated and deplatinated by 0.2 M NaCN for 18 h at 37 °C. After precipitation in ethanol, the deplatinated fragments were migrated on 20% denaturing gel. Their migrations were compared to those of the fragments obtained by partial digestion of the starting oligonucleotide. From their migration, we can determine their length and consequently the platinated base where the 3′-exonuclease stopped its digestion.

CD protocol

CD spectra were recorded on a JASCO J-710 circular dichroism spectropolarimeter using a 10 mm path length quartz cuvette. Scans were performed at controlled temperature (20 °C) over a wavelength range of 210–380 nm (only 240–330 is shown), with a response time of 0.5 s, 1 nm pitch and 1 nm bandwidth. Blank spectra of sample containing buffer were subtracted from collected data. The CD spectra represent an average of five scans and are zero-corrected at 330 nm. Annealed 22AG was used at 3 µM in sodium cacodylate buffer (10 mM, pH 7.4) with 100 mM of KCl or NaCl where appropriate. Quadruplexes were annealed by heating at 90 °C for 5 min and cooled directly to 4 °C to favour the intramolecular folding by kinetic trapping. Concentrations are evaluated by UV measurements (after thermal denaturation for annealed 22AG (5 min at 90 °C)) before use. Each ligand addition step (from 0 to 5 equivalents) is followed by a 5 min equilibration period after which the CD spectrum is recorded.

Biological assay

Preparation of the cells. All cell lines were obtained from the German collection of Microorganisms and Cell Cultures (DSMZ) (Braunschweig, Germany). Adherent cell lines used are: human breast (MCF-7), human bladder (RT-4, 5637), human pancreas (DAN-G) and human lung (A-427, LCLC-103H). Cells were grown in medium containing 90% RPMI 1640 medium (Sigma, Taufkirchen, Germany) and 10% FCS (Sigma), and supplemented with penicillin G/streptomycin. Cell lines were passaged shortly before confluence.

Preparation of the complexes. 1000-fold stock solutions of complexes were prepared in a 1:1 mixture of DMF and water (Millipore-Q; Millipore, Eschborn, Germany). Stock solutions were stored at –30 °C. Immediately prior to testing, stock solutions were removed from the freezer and serially diluted in DMF to

concentrations 500-fold the desired concentrations, giving the series of five dilutions. Two-fold dilutions were done.

Incubation with the complexes. Testing was done with all cell lines growing in 96-well microliter plates. Cells were plated out 24 h prior to testing at a density of 1000 cells/well in 100 μL medium, except for the LCLC-103H cell lines, which was plated out at 500 cells/well in 50 μL medium. At the time, the substances were added to the cells, one untreated plate for each cell line was removed served later as the 'C,0' control (see below). The dilution series of substances were diluted 500-fold into culture medium to give concentrations 2-fold the test concentration. 100 μL of medium containing test substance was added to each well. The final DMF concentrations per drug were 0.1%. Two drugs at five concentrations per drug and eight wells per concentration were tested on each plate. Each plate contained two rows of control wells (i.e. 16 wells). Cells were exposed continuously to all complexes for a period of 96 h.

Evaluating the growth inhibition. The method for measuring growth inhibition of cell lines by Crystal Violet staining has been described in detail elsewhere.[22] Briefly, after a 96-h incubation with substance, the medium was discarded and replaced for 20 min with a 1% glutaraldehyde buffer solution to fix the cells. The fixing solution was discarded and the cells stored under PBS at 4 °C until staining. Staining was done for 30 min with a 0.02% solution of Crystal Violet dissolved in water. After discarding the excess dye and washing the cells for 30 min in water, the cell-bound dye was re-dissolved in 70% ethanol/water and the optical density measured at $\lambda = 570$ nm with an Anthos 2010 plate reader (Anthos, Salzburg, Austria). It should be noted that with the Crystal Violet assay, the cell lines were grown in 200 μL medium, which was sufficient to keep the untreated cells in exponential growth over the 96 h drug exposure time.

Plotting the results. To construct the dose-response curves the corrected T/C values were calculated: $(T/C)_{corr}(\%) = (OD_T - OD_{C,0})/(OD_C - OD_{C,0}) \times 100$, where OD_T is the mean optical density of the treated cells after staining, OD_C is the mean optical density of the controls and $OD_{C,0}$ is the mean optical density at the time the drug was added. The IC_{50} values were estimated by a linear least-squares regression of the T/C_{corr} values *versus* the logarithm of the substance concentration and extrapolating to T/C_{corr} values of 50%; only concentrations that yielded T/C_{corr} values between 10 and 90% were used in calculations.

Acknowledgements

The authors would like to thank Centre National de la Recherche Scientifique (CNRS) and Commissariat à l'Energie Atomique (CEA) for funding H.B., the Association pour la Recherche contre le Cancer (ARC grant 4835 to S.B.) and the E. U. FP6 "MolCancerMed" (LSHC-CT-2004–502943 to J.-L.M.). A De Cian is gratefully acknowledged for preliminary FRET-melting experiments, Drs G. Craescu and S. Miron for the use of CD facilities, M. Bombled for technical assistance with mass spectrometry, and Drs J. Martin and N. Saettel for their help with manuscript correction.

References

1 J. Dai, M. Carver and D. Yang, *Biochimie*, 2008, **90**, 1172; S. Burge, G. N. Parkinson, P. Hazel, A. K. Todd and S. Neidle, *Nucleic Acids Res.*, 2006, **34**, 5402; D. J. Patel, A. T. Phan and V. Kuryavyi, *Nucleic Acids Res.*, 2007, **35**, 7429.
2 A. De Cian, L. Lacroix, C. Douarre, N. Temine-Smaali, C. Trentesaux, J.-F. Riou and J.-L. Mergny, *Biochimie*, 2008, **90**, 131; L. Oganesian and T. M. Bryan, *BioEssay*, 2007, **29**, 155; N. Maizels, *Nat. Struct. Mol. Biol.*, 2006, **13**, 1055; L. Kelland, *Clin. Cancer Res.*, 2007, **13**, 4960.
3 D. Monchaud and M.-P. Teulade-Fichou, *Org. Biomol. Chem.*, 2008, **6**, 627; J. H. Tan, L. Q. Gu and J. Y. Wu, *Mini Rev. Med. Chem.*, 2008, **8**, 1163; A. Arola and R. Vilar, *Curr. Top. Med. Chem.*, 2008, **8**, 1405.
4 J. E. Reed, S. Neidle and R. Vilar, *Chem. Commun.*, 2007, 4366.
5 H. Bertrand, D. Monchaud, A. De Cian, R. Guillot, J.-L. Mergny and M.-P. Teulade-Fichou, *Org. Biomol. Chem.*, 2007, **5**, 2555.
6 D.-L. Ma, C.-M. Che and S.-C. Yan, *J. Am. Chem. Soc.*, 2009, **131**, 1835.
7 R. Kieltyka, J. Fakhoury, N. Moitessier and H. F. Sleiman, *Chem. Eur. J.*, 2008, **14**, 1145.
8 R. Kieltyka, P. Englebienne, J. Fakhoury, C. Autexier, N. Moitessier and H. F. Sleiman, *J. Am. Chem. Soc.*, 2008, **130**, 10040.
9 S. Redon, S. Bombard, M.-A. Elizondo-Riojas and J.-C. Chottard, *Nucleic Acids Res.*, 2003, **31**, 1605; I. Ourliac-Garnier and S. Bombard, *J. Inorg. Biochem.*, 2007, **101**, 514.
10 V. Viglasky, *FEBS J.*, 2009, **276**, 401.
11 I. Ourliac-Garnier, M.-A. Elizondo-Riojas, S. Redon, N. P. Farrell and S. Bombard, *Biochemistry*, 2005, **44**, 10620.
12 H. Bertrand, S. Bombard, D. Monchaud and M.-P. Teulade-Fichou, *J. Biol. Inorg. Chem.*, 2007, **12**, 1003.
13 L. Rao and U. Bierbach, *J. Am. Chem. Soc.*, 2008, **129**, 15764.
14 Y. Jung and S. J. Lippard, *Chem. Rev.*, 2007, **107**, 1387; L. Kelland, *Nat. Rev. Cancer*, 2007, **7**, 573; I. Eryazici, C. N. Moorefield and G. R. Newkome, *Chem. Rev.*, 2008, **108**, 1834; J. Reedijk, *Chem. Rev.*, 1999, **99**, 2499.
15 D. Monchaud, C. Allain, H. Bertrand, N. Smargiasso, F. Rosu, V. Gabelica, A. De Cian, J.-L. Mergny and M.-P. Teulade-Fichou, *Biochimie*, 2008, **90**, 1207.
16 A. De Cian, L. Guittat, M. Kaiser, B. Saccà, S. Amrane, A. Bourdoncle, P. Alberti, M.-P. Teulade-Fichou, L. Lacroix and J.-L. Mergny, *Methods*, 2007, **42**, 183.
17 A. De Cian, P. Grellier, E. Mouray, D. Depoix, H. Bertrand, D. Monchaud, M.-P. Teulade-Fichou, J.-L. Mergny and P. Alberti, *ChemBioChem*, 2008, **9**, 2730.
18 Y. Wang and D. J. Patel, *Structure*, 1993, **1**, 263.
19 J. Dai, M. Carver, C. Punchihewa, R. A. Jones and D. Yang, *Nucleic Acids Res.*, 2007, **35**, 4927; A. T. Phan, V. Kuryavyi, K. N. Luu and D. J. Patel, *Nucleic Acids Res.*, 2007, **35**, 6517.
20 S. Paramasivan, I. Rujan and P. H. Bolton, *Methods*, 2007, **43**, 324; D. M. Gray, J.-D. Wen, C. W. Gray, R. Repges, C. Repges, G. Raabe and J. Fleischhauer, *Chirality*, 2007, **20**, 431; J. Kypr, I. Kejnovska, D. Renciuk and M. Vorlickova, *Nucleic Acids Res.*, 2009, **37**, 1713.
21 Some recent examples: (*a*) E. M. Rezler, J. Seenisamy, S. Bashyam, M.-Y. Kim, E. White, W. D. Wilson and L. H. Hurley, *J. Am. Chem. Soc.*, 2005, **127**, 9439; (*b*) J.-L. Zhou, Y.-J. Lu, T.-M. Ou, J.-M. Zhou, Z.-S. Huang, X.-F. Zhu, C.-J. Du, X.-Z. Bu, L. Ma, L.-Q. Gu, Y.-M. Li and A. S.-C. Chan, *J. Med. Chem.*, 2005, **48**, 7315; (*c*) D. P. N. Goncalves, R. Rodriguez, S. Balasubramanian and J. K. M. Sanders, *Chem. Commun.*, 2006, 4685; (*d*) A. De Cian, E. DeLemos, J.-L. Mergny, M.-P. Teulade-Fichou and D. Monchaud, *J. Am. Chem. Soc.*, 2007, **129**, 1856; (*e*) C. Sissi, L. Lucatello, A. P. Krapcho, D. J. Maloney, M. B. Boxer, M. V. Camarasa, G. Pezzoni, E. Menta and M. Palumbo, *Bioorg. Med. Chem.*, 2007, **15**, 555; (*f*) C.-C. Chang, C. W. Chien, Y.-H. Lin, C.-C. Kang and T.-C. Chang, *Nucleic Acids Res.*, 2007, **35**, 2846; (*g*) D. Monchaud, P. Yang, L. Lacroix, M.-P. Teulade-Fichou and J.-L. Mergny, *Angew. Chem. Int. Ed.*, 2008, **47**, 4858.
22 K. Bracht Boubakari, R. Grünert and P. J. Bednarski, *Anti-Cancer Drugs*, 2006, **17**, 41.
23 S. M. Haider, G. N. Parkinson and S. Neidle, *J. Mol. Biol.*, 2003, **326**, 117; A. T. Phan, V. Kuryavyi, H. Y. Gaw and D. J. Patel, *Nature Chem. Biol.*, 2005, **1**, 167; N. H. Campbell, M. Patel, A. B. Tofa, R. Ghosh, G. N. Parkinson and S. Neidle, *Biochemistry*, 2009, **48**, 1675.